INTERFÉROMÉTRIE OPTIQUE AU SOL ET DANS L'ESPACE
*OPTICAL INTERFEROMETRY AT GROUND LEVEL AND IN SPACE*

# Imaging with multi-aperture optical telescopes and an application

**Gérard ROUSSET, Laurent M. MUGNIER, Frédéric CASSAING, Béatrice SORRENTE**

**Office national d'études et de recherches aérospatiales (ONERA), BP 72, 92322 Châtillon cedex, France**
**E-mail: Gerard.Rousset@onera.fr**

**Abstract.**     The two main types of Multi-Aperture Optical Telescopes (MAOTs) (so-called Michelson and Fizeau) and the two possible modes of optical beam combination are reviewed. Wide-field imaging with a Michelson instrument is studied and the constraints are identified. An example of application to Earth observation is given. Then, we address the optimization of the aperture configuration, a key issue in the design of a MAOT. We also stress the image restoration, a necessary component of such an instrument because of the shape of its point spread function. Finally, a MAOT seems to be a promising technical solution for high resolution Earth observation from Space on a high orbit such as a geostationary one. © 2001 Académie des sciences/Éditions scientifiques et médicales Elsevier SAS

**optical interferometry / imaging / synthetic aperture optics / phased array telescope / high angular resolution**

### *Imagerie par télescopes optiques multi-pupilles et application*

**Résumé.**     *Les deux types de télescopes optiques multi-pupilles (appelés Michelson et Fizeau) et les deux modes possibles de recombinaison des faisceaux optiques sont présentés. L'imagerie grand champ avec un instrument Michelson est étudiée et les contraintes identifiées. Un exemple d'application à l'observation de la Terre est donné. Ensuite, nous abordons l'optimisation de la configuration pupillaire, un point-clef dans la conception d'un télescope multi-pupille. Nous insistons aussi sur le traitement d'images, une composante nécessaire d'un tel instrument à cause de la forme de sa fonction d'étalement de point. Finalement, le télescope optique multi-pupille semble être une solution technique prometteuse pour l'observation de la Terre à haute résolution à partir de l'Espace sur une orbite haute comme l'orbite géostationnaire. © 2001 Académie des sciences/Éditions scientifiques et médicales Elsevier SAS*

***interférométrie optique / imagerie / synthèse d'ouverture optique / réseau de télescopes phasés / haute résolution angulaire***

## 1. Introduction

The resolution of a diffraction limited optical telescope is given by $\lambda/D$ where $D$ is its diameter and $\lambda$ the observation wavelength. Today, this diameter is limited by the current technology to about 10 meters

for ground-based systems, and even more limited by volume and mass constraints for space-based systems. The Multiple Aperture Optical Telescope (MAOT) is a technical solution that allows the breaking of this limit. It consists in making an array of elementary telescopes (or of mirror segments) interfere, so that the measured data contains some high resolution information at spatial frequency $B/\lambda$. $B/\lambda$ is given by the separation $B$ (or 'baseline') of the elementary telescopes rather than by their diameters. This technique may generate an equivalent instrument of pupil diameter $B$, even with some holes in the pupil area coverage.

Today on the ground, such arrays have baselines of the order of a few hundred meters and are made of a few independent elementary telescopes of diameter varying from ten centimeters to ten meters [1]. They are called interferometers because the measured data are usually the visibilities of the fringes produced by pairs of elementary telescopes. The visibility corresponds to the amplitude of the object spectrum at the spatial frequency $B/\lambda$. During an observation run, only very few discrete object spectrum values are collected. In space, such interferometers are at the project stage [2,3]. In this paper, we want to present another type of instrument using some principles of these interferometers but providing direct images of the object in a wide field of view.

In Section 2, we discuss the typology of MAOTs in terms of optical design and beam combination scheme. In Section 3, we investigate the capability of a MAOT to provide wide field images for very extended objects. An example of application is given in Section 4. Then in Section 5, we study the optimization problem of the array configuration in order to maximize the performance of the instrument. In Section 6, the image restoration problem is discussed and simulation results are presented.

## 2. Typology of multi-aperture optical telescopes

Two main types of MAOT can be distinguished (see *figure 1*, from [4]). The Fizeau interferometer contains a set of mirror segments defining subapertures and forming a virtually common primary mirror, whose light is combined onto a common secondary mirror (which can itself be segmented). The combination of the light beams coming from each piece of the primary mirror forms an image that is recorded in a common focal plane, in exactly the same way as for a monolithic telescope. One key issue is the phasing of all the segments of the virtual primary mirror. It consists in the compensation for the piston, tip and tilt of each segment up to an accuracy better than $\lambda/10$ in order to achieve the diffraction limit of the Fizeau interferometer. Each of the two Keck telescopes [5], the next generation space telescope (NGST) [6] and the extremely large telescope concepts [7] are examples of such an instrument (having a filled pupil area).

In contrast, the Michelson interferometer consists of a set of elementary telescopes (defining subapertures), whose light is brought by a set of periscopes into a so-called beam combination interferometer. The interferences can be recorded either in a pupil plane or in a focal plane. The ground-based interferometers
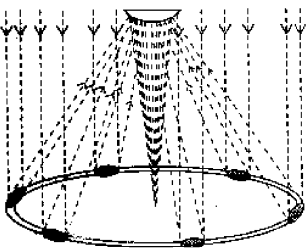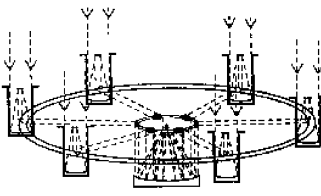


| Fizeau | Michelson |
| --- | --- |
| Common virtual primary | Elementary telescopes |
| Focal plane combination: ⇒ image formation | Periscopes + interferometer: pupil or focal plane detection |

**Figure 1.** The two types of MAOT (from [4]).

built or being built for astronomy are Michelson-type interferometers (see, for instance, [1] and [8]). These interferometers have independent elementary telescopes pointing the object. Therefore long delay lines, of stroke comparable to the baseline length, are required to acquire and track the null optical path difference (OPD) between the elementary telescopes. But in the case of baselines smaller than 100 m, we can also imagine using a unique mechanical structure to support all the elementary telescopes and point the object, suppressing the need for long delay lines [9]. We will discuss such a concept in the next section. In such a case, one advantage of the Michelson instrument is its compactness: its volume roughly varies as the square of the baseline while for a Fizeau it varies as the cube because the distance between the primary mirror segments and the common secondary is of the order of the primary mirror diameter.

There are two main modes for the beam combination: in the pupil plane or in the focal plane. In the pupil plane combination mode, the subaperture images of two elementary telescopes are superimposed to form flat tint interferences. The fringe pattern is recorded by only one detector (per spectral channel) using an OPD modulation [10]. The visibility is measured at the spatial frequency $B/\lambda$. Note that a more sophisticated technique, rotational shearing interferometry [11], could give access to a much larger number of frequencies, to be recorded by a detector array which samples the superimposed rotated pupil images. In the pupil plane mode, there is no direct imaging of the object. The object reconstruction usually results from a model fitting to the collected visibilities. If necessary, an image can be synthesized by Fourier transform techniques but these must take care of the field aliasing problem due to the sampling of the spatial frequency plane. Only a distribution of discrete visibilities is available in this plane. This problem is similar to the one encountered in synthetic aperture radioastronomy [12]. Therefore, the observed object must be very small. Its maximum size is related to the pupil sampling and is at most $\lambda/B_{\min}$ where $B_{\min}$ is the minimum baseline defined by the elementary telescope array.

In the focal plane combination mode, the object images produced by each elementary telescope are superimposed. Within the isoplanatic field, the formed fringe patterns can be interpreted as a convolution of the object by the Point Spread Function (PSF) of the instrument. Compared to the monolithic telescope case, the MAOT PSF may have a very large number of sidelobes (superimposition of fringe patterns). However, these lobes are attenuated by their envelope which is the elementary telescope PSF. Therefore, the image does not contain any field aliasing of the object because the interferometer PSF is not periodic. Because of the extent of each subaperture (corresponding to each elementary telescope), a continuum of frequencies around the spatial frequency $B/\lambda$ can be recorded in the image, without any sampling limitation in the spatial frequency plane.

## 3. Wide-field imaging with a multi-aperture optical telescope

The Fizeau-type instrument is intrinsically an imager and has a wide field of view (FOV), which is limited by the aberrations of the optical design in much the same way as for a monolithic telescope. The Michelson-type instruments are usually not designed to produce direct images. In particular, when the data are recorded in a pupil plane, only a discrete set of spatial frequencies of the object spectrum (visibilities) is recorded. The FOV is then very limited (risk of field aliasing). In order for a Michelson to produce wide field images, it is necessary to record an image in a focal plane, so that a continuum of spatial frequencies is recorded and a wide field may be accessible.

Let us give the conditions under which wide FOV imaging is feasible with a Michelson. It is always possible to cophase at any field position the elementary telescopes of an array by adjusting the delay lines (OPD control) and the tip/tilt mirrors, included in the periscopes for example. The overall wavefront accuracy to achieve this must be better than $\lambda/10$. For large field imaging, accurate cophasing should be simultaneously ensured over the whole FOV, not only on-axis. The effect of these new constraints has been evaluated [10]. As expected, it can be shown that the cophasing complexity (i.e. the number of optical parameters to control) increases with the field to resolution ratio (FRR), which is the number of resolved elements in the desired field. The results are summarized in the *table*, which includes the beam combination and the optical design constraints.

**Table.** Complexity of an imaging Michelson-type instrument as a function of the field to resolution ratio (FRR)

| FRR | Optical constraints |
| --- | --- |
| $\approx 1$ | on-axis OPD and tip/tilt control |
| $\approx 10$ | + lateral baseline homothecy |
| $\approx 100$ | + full (baseline + diameter) lateral homothecy |
| $\geqslant 1000$ | + longitudinal homothecy + field curvature and distortion. |

For the beam combination constraints, a famous requirement is the lateral homothetic pupil mapping, known as the 'golden rule' of multi-aperture optics [13]: the exit pupil after the elementary telescopes and periscopes should be an exact demagnified replica of the input pupil. This requirement is sufficient for most the astronomical applications (FRR $\approx 100$). However for a smaller field (FRR $\approx 10$), the subaperture demagnification by the elementary telescopes can differ from the baseline demagnification by the periscopes, leading to the 'densified pupil' concept as introduced by Labeyrie [14]. For a larger FOV (FRR $\approx 1000$), longitudinal pupil homothecy must also be considered [15]. For even larger FOV, the subapertures must be coplanar. Besides, additional constraints are put on the optical design of the elementary telescopes. Considering afocal elementary telescopes of revolution, they must successively have matched magnifications, be aplanatic [16] and have a sine-law distortion [17], when increasing the FOV from a FRR $\approx 100$ up to 10000.

## 4. Application to Earth observation

This analysis has been applied in a feasibility study on Earth observation with a MAOT. A conceptual design was performed considering a Michelson-type instrument having three elementary telescopes, supported and pointed by a unique mechanical structure to avoid large stroke delay lines. The beam combination is made in a focal plane. A perspective view of the instrument is shown in *figure 2*. In the box at the left of the three elementary telescopes is the off-axis beam combiner.

A thorough simulation of this instrument has been performed, whose results are given in Section 6. In particular, tests performed with an optical design software confirmed that by careful design of the elementary telescopes, the requirements for a very large FRR can be fulfilled. For instance, the relevant
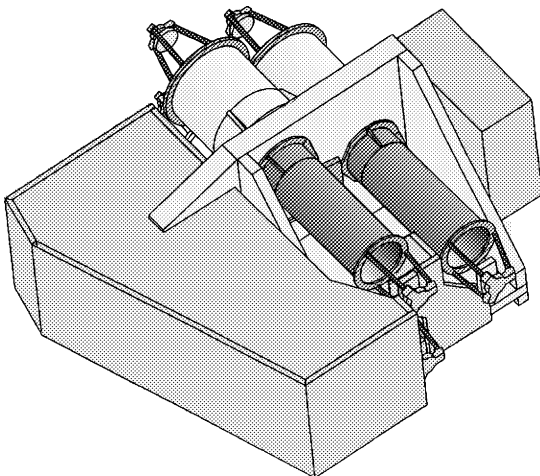


**Figure 2.** Perspective view of a MAOT for Earth observation (courtesy of *SpaceBel* instrumentation).

distortion was introduced in the design of the elementary telescopes. In addition, each periscopic mirror was mounted on three linear actuators in order to control for each beam OPD, tip, tilt and pupil position.

Cophasing such an instrument is a major issue because of the large number of degrees of freedom. The proposed strategy uses an on-board artificial source and the observed object itself to measure the phase perturbations introduced by the vibrations and the thermal drifts on the satellite. The most critical parameters to be controlled in real-time are on-axis OPD and tip/tilt on each subaperture. They are measured by the on-board source sensor; this sensor analyzes the diffraction pattern of the 3-beam interferogram given by a point-like artificial source retro-reflected by a common reference plane, which overlaps a small area of each subaperture [18]. This setup ensures fast and accurate measurements to correct for instrument vibrations, but can be biased by aperture undersampling or by reference drifts.

The other parameters to be controlled in real-time are the lateral and longitudinal subaperture positions and the elementary telescope magnification. Measuring these parameters requires sensors distributed in the whole FOV. Fortunately these parameters are less critical in terms of amplitude and can be measured at a lower frequency, directly on the observed object in order to minimize biases. To measure OPDs on extended objects, the sensors are based on spatial filtering with a monomode fiber. For the tip/tilt control, correlation trackers are proposed. These so-called external sensors are also used to correct for the slowly evolving bias of the on-board source sensor.

## 5. Aperture configuration optimization

The choice of the positioning of the elements of a phased array of optical telescopes is an important point for the preliminary design of a MAOT, whether these elements be pieces of a primary mirror (Fizeau) or elementary telescopes (Michelson). A whole body of work exists in the literature on this subject, either based on shaping the PSF of the instrument, or on the idea of uniformity of the frequency coverage.

A more global approach consists in considering together the image acquisition and the restoration, and in optimizing the aperture configuration so that the restored image be as close as possible to the original observed object. Let $o$ be the original object of interest, and $i = h \star o + n$ the recorded image, where $h$ is the PSF of the instrument, $\star$ denotes convolution and $n$ is an additive noise. In order to keep the derivations tractable, the deconvolution is taken as a linear filter $g$ (e.g., an inverse filter truncated to the maximum spatial frequency of interest); the restored image, or estimated object, is then $\hat{o} = g \star i$. If nothing is assumed about the noise statistics, then it can be shown [19] that the aperture configuration that leads to an $\hat{o}$ that is closest to $o$ in the least-squares sense is the one that maximizes the minimum of the transfer function $\tilde{h}$ over the frequency domain of interest. One can note that this result gives a frequency-domain optimality condition, but this condition is not imposed a priori but, rather, derived from the described global approach, which considers the image restoration as part of the observation system.

*Figure 3* shows the result of this optimization performed for 3, 4 and 5 elementary telescopes, for a given collecting surface and a given target resolution. The collecting surface is derived from signal-to-noise ratio considerations, and the maximum frequency of interest is derived from mission requirements. One can notice in particular that the four elementary telescopes optimal configuration is not a square, which ensures a better frequency coverage.



**Figure 3.** Optimal aperture configurations with 3, 4 and 5 elementary telescopes, for a given collecting surface and resolution.

## 6. Image simulation and restoration

Due to the peculiar shape of the PSF of a MAOT, image restoration is a necessary component of the observation system. The data processing is similar to that of images taken by monolithic telescopes. The above-mentioned Earth observation MAOT has been simulated. Its transfer function (see *figure 4*) is lower than for a monolithic telescope, but does not go down to zero in the frequency domain of interest with the aperture configuration optimized as described in the previous section. The optical transfer function includes design, fabrication and assembly aberrations, as well as cophasing residuals. The simulation also takes into account the detector transfer function as well as photon and detector noises. The top part of *figure 4* shows the used object and the noisy image formed by the simulated instrument.

It is well known that the restoration of the object using the sole data is an unstable process [20]. It is therefore necessary to add a priori information on the solution into the restoration method. This can be done in a Maximum A Posteriori (MAP) framework: the object is endowed with an a priori distribution $p(o)$, and Bayes' rule combines the likelihood of the data $p(i|o)$ with this a priori distribution into the a posteriori probability distribution $p(o|i)$. If the PSF $h$ is perfectly known, then the restored object can be defined as the most probable one given the data: $\hat{o}_{\mathrm{map}} = \arg\max_o(p(o|i)) = \arg\max_o(p(i|o) \times p(o))$. The prior information on the object that is incorporated into $p(o)$ is the available statistical knowledge on its spatial structure, its positivity and possibly its support. With gaussianity and stationarity assumptions both
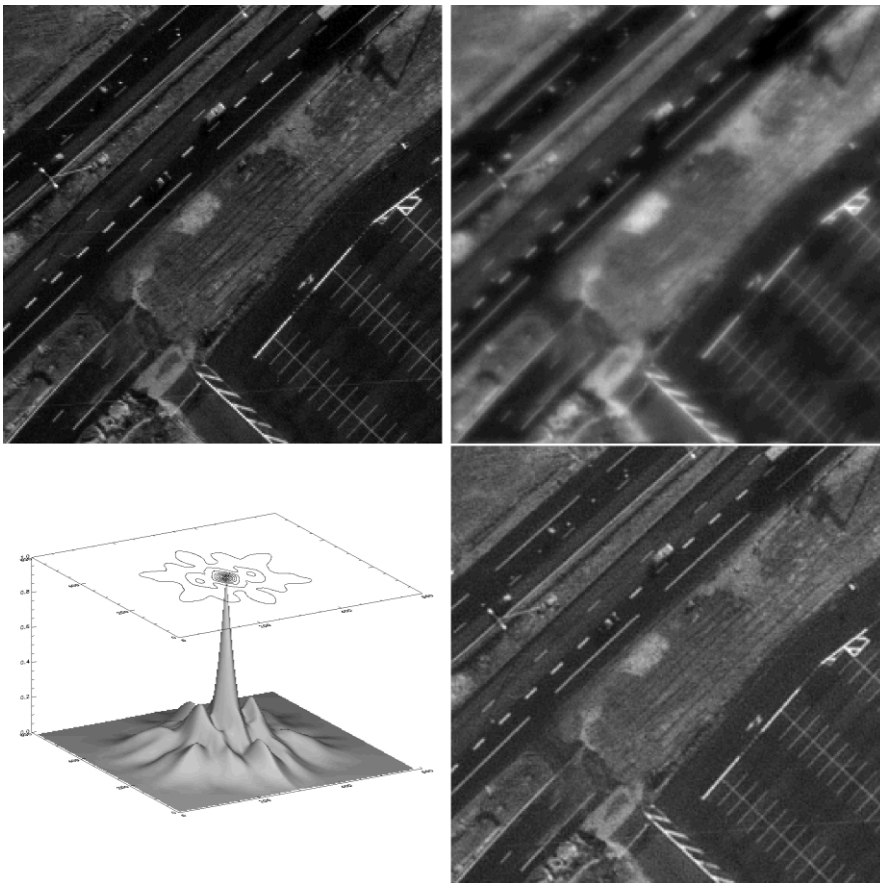


**Figure 4.** Object used for the simulation (top left), simulated noisy image (top right), transfer function in perspective view (bottom left) and restored image (bottom right).
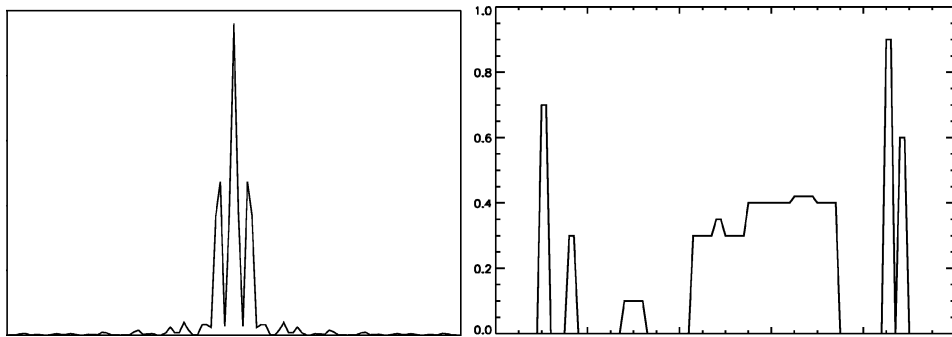
**Figure 5.** PSF of a diluted two-telescope instrument, and object considered for the simulation.
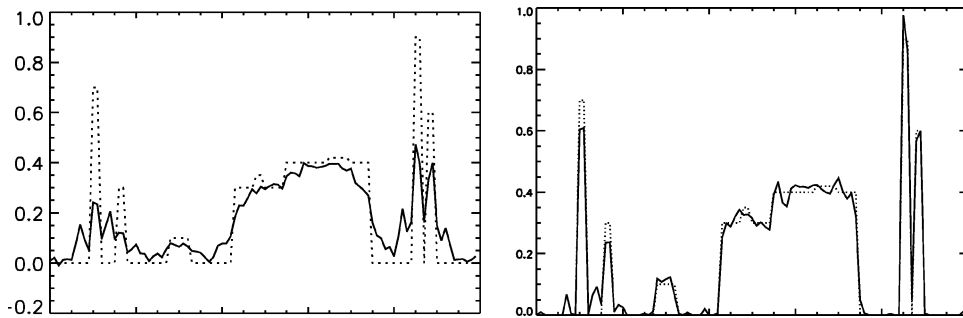


**Figure 6.** Simulated (left) and restored (right) images. The true object is recalled in dotted line.

on the object and on the noise, this maximization has an analytical solution, which is the well-known Wiener filter estimate. This estimate is shown in the bottom part of *figure 4*; the prior information used consists of a parametric model for the Power Spectral Density (PSD) of the object [21] and the noise variance, which can both be estimated from the image itself by, e.g., the maximum likelihood method. This simulation and restoration have been used to validate the instrument design.

If one wants to put such a MAOT into a high altitude orbit and to keep a high resolution, the size and/or the number of elements of the phased array must be increased. In order to keep these reasonably small, it is worth investigating the possibility to perform some spectral extrapolation from the image, i.e., to restore spatial frequencies that have not been recorded by the instrument. It can be shown that if the models for the object prior probability and for the noise are stationary and Gaussian, such an extrapolation is impossible; indeed, the restored image is then a linearly filtered version of the recorded image. One must then resort to more advanced, non-linear restoration methods, which introduce non-gaussianity in the prior (e.g., edge-preserving priors [22–24], entropic priors, etc.) and/or non-stationarity (e.g., object support information). This has been validated on a one-dimensional simulation of a MAOT; *figure 5* shows the PSF (left) corresponding to a two-telescope instrument having zeros before the cutoff frequency in its transfer function and the considered object (right), which has a combination of smooth areas and spikes.

The left part of *figure 6* shows the image that would be recorded by such an instrument, with a 1% additive noise. The right part of *figure 6* shows the restored images obtained with an edge-preserving prior and a prior on the bounds of the object (constrained to be between 0 and 1). The object is quite well restored despite the missing frequencies in the recorded image. The inspection of the Fourier transform of the restored object (continuous line in *figure 7*) shows that the missing frequencies in the transfer function (dashed line) have indeed been restored by the use of the edge-preserving prior. One must note that this spectral interpolation (and extrapolation) works well only when the size of the frequency holes to be filled in is relatively small
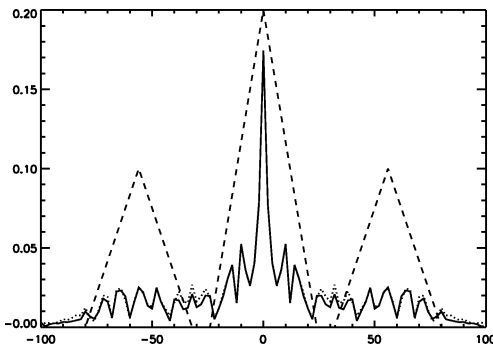
**Figure 7.** Spectrum of the restored image (continuous line); the spectrum of the true object (dots) and the transfer function (dashed line) are shown for comparison.

compared to the overall frequency domain of interest [25]. When it is not the case, we find that the object frequencies lying between the central peak and the interference peak are notably underestimated.

Another advanced image restoration problem of interest for a MAOT is the case when the instrument is not perfectly calibrated and the PSF is imperfectly known; this may be due for instance to thermal dilation or vibration residuals after cophasing. A solution to this problem is known as 'myopic deconvolution'; it consists in jointly estimating the object of interest and the PSF; this has already been demonstrated for long exposure images in adaptive optics [21,23], for short exposures in speckle imaging [26] and in deconvolution by wavefront sensing [24]. This myopic deconvolution gives good results provided one has some information on the PSF and its variability, in order to sufficiently constrain the estimation. For long exposures, this information is for instance the average and the PSD of the PSF (i.e., error bars on the transfer function) [21]. For short exposures, an efficient way to constrain the estimation is to model the PSF through the instantaneous phase in the pupil [26,24]. This approach should be compared to the phase closure technique developed in interferometry with very diluted apertures.

## 7. Conclusion

We have studied the problem of wide-field imaging with a MAOT. Wide-field imaging is possible both for a Fizeau and for a Michelson instrument, a necessary condition being the recording of the data in the focal plane (image) and not in a pupil plane (visibilities). In particular, the constraints on the beam combination and the optical design are detailed for a Michelson. These results were used in the design of a Michelson MAOT for Earth observation, where wide field cophasing is required. The proposed cophasing strategy uses both an on-board artificial source and the object itself in order to measure and control all the required phase parameters. We have developed a tool taking into account the image post-processing for the optimization of the aperture configuration. We have simulated the whole acquisition and processing chain for the given example of a MAOT dedicated to Earth observation. We have also mentioned some possibilities for the processing of images coming from a diluted aperture instrument or from an imperfectly calibrated instrument.

Therefore, we believe that the MAOT should be a very promising technical solution for Earth observation from Space on a high-altitude orbit. In particular a MAOT on a geostationary orbit would allow the permanent monitoring of a given zone while having a resolution comparable to that of current low Earth orbit satellites.

As a final note, we would like to point out that in the course of this work, it has become more and more apparent that even the early design of the instrument must incorporate the data post-processing as a key subsystem of the global observing system, because this processing can have a strong impact on the design solutions.

## References

[1] Glindemann A., Abuter R., Carbognani F., Delplancke F. et al., The VLTI interferometer, C.R. Acad. Sci. Paris Sér. IV 2 (1) (2001) 57–65, this volume.

[2] Shao M., Wolff D.M., Orbiting stellar interferometer, in: R.D. Reasenberg (Ed.), Spaceborne Interferometry II, Proc. Soc. Photo-Opt. Instrum. Eng., Vol. 2477, 1995, pp. 228–239.

[3] Lund G., Bonnet H., The Darwin project: space interferometry, C.R. Acad. Sci. Paris Sér. IV 2 (1) (2001) 137–148, this volume.

[4] Faucherre M., Merkle F., Vakili F., Beam combination in aperture synthesis from space: Field of view limitations and $(u, v)$ plane coverage optimization, in: J.-P. Swings (Ed.), New Technologies for Astronomy, Proc. Soc. Photo-Opt. Instrum. Eng., Vol. 1130, April 1989, pp. 138–145.

[5] Nelson J.E., Mast T.S., Construction of the Keck Observatory, in: M.-H. Ulrich (Ed.), Very Large Telescopes and their Instrumentation, ESO Conference Proceedings, Vol. 30, ESO, Garching, Germany, 1988, pp. 7–14.

[6] Bely P.-Y., The NGST "yardstick mission", in: The Next Generation Space Telescope: Science Drivers and Technological Challenges, Liège, Belgium, June 1998, ESA SP-429, pp. 159–166.

[7] Gilmozzi R., Delabre B., Dierickx P., Hubin N., Koch F., Monnet G., Quattri M., Rigaut F., Wilson R.N., The future of filled aperture telescopes: is a 100 m feasible?, in: Advanced Technology Optical/IR Telescopes VI, Proc. Soc. Photo-Opt. Instrum. Eng., Vol. 3352, 1998, pp. 778–791.

[8] Mourard D., Thureau N., Abe L., Berio P. et al., The GI2T/Regain Interferometer, C.R. Acad. Sci. Paris Sér. IV 2 (1) (2001) 35–44, this volume.

[9] Meinel A.B., Shannon R.R., Whipple F.L., Lox F.J., A large multiple mirror telescope (MMT) project, Opt. Eng. 11 (2) (1972) 33–37.

[10] F. Cassaing, Analyse d'un instrument à synthèse d'ouverture optique : méthodes de cophasage et imagerie à haute résolution angulaire, PhD thesis, Université Paris XI, Orsay, 1997.

[11] Roddier C., Roddier F., High angular resolution observations of Alpha Orionis with a rotation shearing interferometer, Astrophys. J. 270 (1983) L23–L26.

[12] Lannes A., Anterrieu E., Bouyoucef K., Fourier interpolation and reconstruction via Shannon-type techniques, part I: Regularization principle, J. Mod. Opt. 41 (1994) 1537.

[13] Traub W.A., Combining beams from separated telescopes, Appl. Opt. 25 (4) (1986) 528–532.

[14] Labeyrie A., Resolved imaging of extra-solar planets with future 10–100 km optical interferometric arrays, Astron. Astrophys. Suppl. Ser. 118 (1996) 517–524.

[15] Beckers J.M., The VLT Interferometer III. Factors affecting wide field-of-view operation, in: L.D. Barr (Ed.), Advanced Technology Optical Telescopes IV, Part I, Proc. Soc. Photo-Opt. Instrum. Eng., Vol. 1236, 1990, pp. 379–389.

[16] Harvey J.E., Ftaclas C., Field-of-view limitations of phased telescope arrays, Appl. Opt. 34 (25) (1995) 5787–5798.

[17] Stuhlinger T.W., All-reflective phased array imaging telescopes, in: International Lens Design Conference, Proc. Soc. Photo-Opt. Instrum. Eng., Vol. 1354, 1990, pp. 438–446.

[18] Cassaing F., Mugnier L.M., Rousset G., Sorrente B., Key aspects in the design of a synthetic aperture optics space telescope for wide field imaging, in: N. Duric (Ed.), Catching the Perfect Wave, Publ. Astron. Soc. Pac., Vol. 174, Albuquerque, June 1998.

[19] Mugnier L.M., Rousset G., Cassaing F., Aperture configuration optimality criterion for phased arrays of optical telescopes, J. Opt. Soc. Am. A 13 (12) (1996) 2367–2374.

[20] Demoment G., Image reconstruction and restoration: Overview of common estimation structures and problems, IEEE Trans. Acoust. Speech Signal Process. 37 (12) (1989) 2024–2036.

[21] Conan J.-M., Mugnier L.M., Fusco T., Michau V., Rousset G., Myopic deconvolution of adaptive optics images using object and point spread function power spectra, Appl. Opt. 37 (21) (1998) 4614–4622.

[22] Green P.J., Bayesian reconstructions from emission tomography data using a modified EM algorithm, IEEE Trans. Med. Imag. 9 (1990) 84–93.

[23] Conan J.-M., Fusco T., Mugnier L.M., Kersalé E., Michau V., Deconvolution of adaptive optics images with imprecise knowledge of the point spread function: results on astronomical objects, in: D. Bonaccini (Ed.), Astronomy with Adaptive Optics: Present Results and Future Programs, ESO/OSA, Vol. 56, ESO, Garching bei München, Germany, February 1999, pp. 121–132.

[24] Mugnier L.M., Robert C., Conan J.-M., Michau V., Salem S., Myopic deconvolution from wavefront sensing, J. Opt. Soc. Am. A, à paraître.

[25] Lannes A., Roques S., Casanove M.-J., Stabilized reconstruction in image and signal processing; part I: Partial deconvolution and spectral extrapolation with limited field, J. Mod. Opt. 34 (2) (1987) 161–226.

[26] Schulz T.J., Multiframe blind deconvolution of astronomical images, J. Opt. Soc. Am. A 10 (5) (1993) 1064–1073.